ACCOUNTS of chemical research

pubs.acs.org/accounts
Article

Modulating the Photophysical Properties of Twisted Donor–Acceptor–Donor π-Conjugated Molecules: Effect of Heteroatoms, Molecular Conformation, and Molecular Topology

Youhei Takeda*

Cite This: *Acc. Chem. Res.* 2024, 57, 2219–2232
Read Online

CONSPECTUS: Modulating the photophysical properties of organic emitters through molecular design is a fundamental endeavor in materials science. A critical aspect of this process is the control of the excited-state energy, which is essential for the development of triplet exciton-harvesting organic emitters, such as those with thermally activated delayed fluorescence and room-temperature phosphorescence. These emitters are pivotal for developing highly efficient organic light-emitting diodes and bioimaging probes. A particularly promising class of these emitters consists of twisted donor–acceptor organic π-conjugated scaffolds. These structures facilitate a spatial separation of the frontier molecular orbitals, which is crucial for achieving a narrow singlet–triplet energy gap. This narrow gap is necessary to overcome the endothermic reverse intersystem crossing process, enhancing the efficiency of thermally activated delayed fluorescence. To precisely modulate the photophysical properties of these emitting materials, it is essential to understand the electronic structures of new donor–acceptor scaffolds, especially those influenced by heteroatoms, as well as their conformations and topologies. This understanding not only improves the efficiency of these emitters but also expands their potential applications in advance technologies.

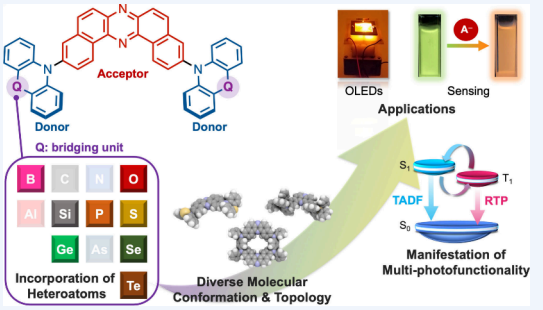

In 2014, the Takeda group made a significant breakthrough by discovering a novel method for synthesizing U-shaped diazaacenes (dibenzo[*a,j*]phenazine) through an oxidative skeletal rearrangement of 1,1′-binaphthalene-2,2′-diamines. This class of compounds is typically challenging to synthesize using conventional organic reactions. The resulting unique geometric and electronic structure of U-shaped diazaacenes opened new possibilities for photophysical applications. Leveraging the U-shaped structure, photoluminescent properties, and high electron affinity, we developed twisted donor–acceptor–donor compounds. These compounds exhibit efficient thermally activated delayed fluorescence, stimuli-responsive luminochromism, heavy atom-free room-temperature phosphorescence, and anion-responsive red shifts. These innovative emitters have demonstrated significant potential in various practical applications, including organic light-emitting diode devices and advanced sensing systems.

In this Account, I summarize our achievements in modulating the photofunctions of dibenzo[*a,j*]phenazine-cored twisted donor–acceptor–donor compounds by controlling excited-state singlet–triplet energy gaps through conformational regulation. Our comprehensive studies revealed the significant impact of heteroatoms, molecular conformations, and topologies on the photophysics of these compounds. These findings highlight the importance of molecular engineering in tailoring the photophysical properties of organic donor–acceptor π-conjugated materials for specific applications. Our research has demonstrated that incorporating heteroatoms into the molecular framework effectively tunes the electronic properties and, consequently, the photophysical behavior of the compounds. Understanding the influence of heteroatoms, conformational dynamics, and molecular topology on excited-state behavior will open new avenues for next-generation optoelectronic devices and biological technologies. These advancements include ultra-low-power displays, photonic communication, and super-resolution biomedical imaging. Ultimately, our work highlights the potential of strategic molecular design in driving innovation across various fields, paving the way for the development of cutting-edge technologies that leverage the unique properties of organic emitters.

KEY REFERENCES

- Data, P.; Pander, P.; Okazaki, M.; Takeda, Y.; Minakata, S.; Monkman, A. P. Dibenzo[*a,j*]phenazine-Cored Donor-Acceptor-Donor Compounds as Green-to-Red/NIR Thermally Activated Delayed Fluorescence Organic Light Emitters. *Angew. Chem. Int. Ed.* **2016**, *55*, 5739–

Received: June 6, 2024
Revised: July 13, 2024
Accepted: July 16, 2024
Published: July 24, 2024

https://doi.org/10.1021/acs.accounts.4c00353
Acc. Chem. Res. 2024, 57, 2219–2232

5744.[1] *The first twisted photofunctional dibenzo[a,j]-phenazine-cored donor−acceptor−donor compounds were developed. Organic light-emitting diodes fabricated with a donor−acceptor−donor compound as the emitter displayed efficient orange thermally activated delayed fluorescence with a high external quantum efficiency of up to 16%.*

- Okazaki, M.; Takeda, Y.; Data, P.; Pander, P.; Higginbotham, H.; Monkman, A. P.; Minakata, S. Thermally Activated Delayed Fluorescent Phenothiazine-Dibenzo[*a,j*]phenazine-Phenothiazine Triads Exhibiting Tricolor-Changing Mechanochromic Luminescence. *Chem. Sci.* **2017**, *8*, 2677−2686.[2] *The first thermally activated delayed fluorescence-active, multi-color-changing mechanochromic organic material was developed by leveraging the conformational flexibility of a twisted donor−acceptor−donor molecule. The study revealed the significant impact of incorporating a sulfur atom in the donor on mechanochromism.*
- Izumi, S.; Higginbotham, H. F.; Nyga, A.; Stachelek, P.; Tohnai, N.; de Silva, P.; Data, P.; Takeda, Y.; Minakata, S. Thermally Activated Delayed Fluorescent Donor-Acceptor-Donor-Acceptor π-Conjugated Macrocycle for Organic Light-Emitting Diodes. *J. Am. Chem. Soc.* **2020**, *142*, 1482−1491.[3] *The first macrocyclic thermally activated delayed fluorescence organic molecule serving as an organic light-emitting diode emitter was developed. This study revealed the impact of molecular topology (cyclic versus linear) on thermally activated delayed fluorescence efficiency.*
- Aota, N.; Nakagawa, R.; de Sousa, L. E.; Tohnai, N.; Minakata, S.; de Silva, P.; Takeda, Y. Anion-Responsive Colorimetric and Fluorometric Red-Shift in Triarylborane Derivatives: Dual Role of Phenazaborine as Lewis Acid and Electron Donor. *Angew. Chem. Int. Ed.* **2024**, *63*, e202405158.[4] *Donor−acceptor−donor compounds that exhibit an anion-responsive significant colorimetric and fluorometric red shift in both solution and solid states were successfully developed through balancing the contradictory roles of phenazaborine as a Lewis acid and as an electron donor.*

INTRODUCTION

Organic π-conjugated donor−acceptor (D−A) compounds have played pivotal roles in contemporary science, leading to a multitude of applications including organic photovoltaics,[5] organic field-effect transistors,[6] and photocatalysis.[7] Notably, the past decade has seen remarkable progress in D−A-type organic emitters exhibiting thermally activated delayed fluorescence (TADF).[8] TADF is a crucial photophysical phenomenon wherein triplet excitons are thermally converted to singlet excitons via reverse intersystem crossing (RISC), leading to delayed emission from the resultant singlet excitons (Figure 1a).[9] To facilitate the endothermic RISC process and expedite the typically forbidden spin-flipping, the energy gap (ΔE_{ST}) between the singlet excited state (S_1) and triplet excited state (T_n) must be narrow (ΔE_{ST} < 0.3 eV), and spin-orbit coupling (SOC) should be substantial.[10,11] TADF-active organic molecules can theoretically achieve 100% quantum efficiency in converting electronically generated excitons into light, without relying on rare metals such as Ir and Pt. Consequently, TADF organic compounds have emerged as the third generation of emitters for efficient organic light-emitting diodes (OLEDs).[12,13] The rediscovery of these advanced emissive

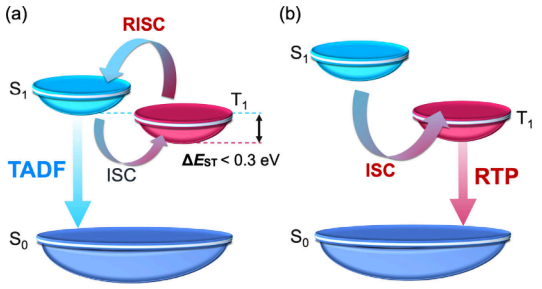

Figure 1. Illustrative schemes for (a) TADF and (b) RTP.

materials has significantly enhanced the efficiency of OLEDs and spurred the development of novel biological technologies.[14]

Room-temperature phosphorescence (RTP), another significant photophysical phenomenon, has garnered substantial interest due to its fundamental importance and wide-ranging applications.[15−17] Since RTP arises from the triplet excited state (Figure 1b), which also serves as an intermediate for TADF, the photophysical behavior of organic molecules displaying TADF and/or RTP is highly dependent on ΔE_{ST} and SOC. By fine-tuning molecular parameters such as atomic composition and three-dimensional molecular geometry, it is possible to enhance specific photofunctions or induce multiple photofunctions, including TADF/RTP switching, within a single D−A molecular scaffold. TADF and RTP typically exhibit distinct emission colors and show opposite thermal response. Consequently, TADF/RTP switching could be highly beneficial for applications such as thermochromic luminescence displays. This paves the way for next-generation organic photofunctional materials.[18] A thorough understanding of the intricate electronic structures of new D−A scaffolds, influenced by heteroatoms within conjugated frameworks along with their molecular conformations and topologies, is essential for the precise modulation of photophysical properties in π-conjugated scaffolds.

In 2014, we discovered a novel oxidative skeletal rearrangement of 1,1′-binaphthalene-2,2′-diamines and developed a synthetic method to access U-shaped dibenzo[*a,j*]phenazines (DBPHZ), a compound class that is challenging to synthesize through conventional organic reactions (Scheme 1).[19] These newly synthesized aza-polycyclic hydrocarbon molecules feature a distinct U-shaped structure,[19] photoluminescent properties,[19,20] and high electron affinities.[19] Leveraging the electron-deficient and luminescent characteristics and halogeno functionality introduced at the periphery of the DBPHZ, we have developed a diverse array of DBPHZ-cored D−A−D

Scheme 1. Oxidative Skeletal Rearrangement of 1,1′-Binaphthalene-2,2′-diamines

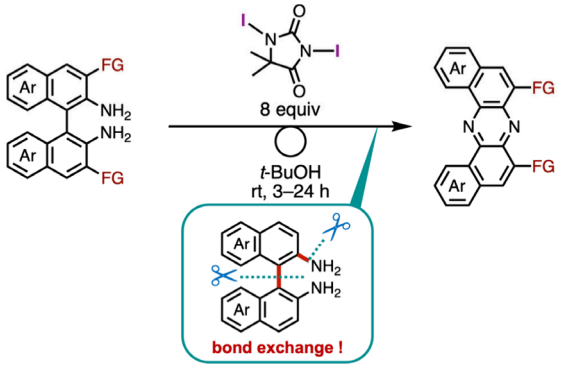

https://doi.org/10.1021/acs.accounts.4c00353
Acc. Chem. Res. 2024, 57, 2219−2232

Scheme 2. General Synthetic Route to Twisted DBPHZ-Cored D−A−D Compounds

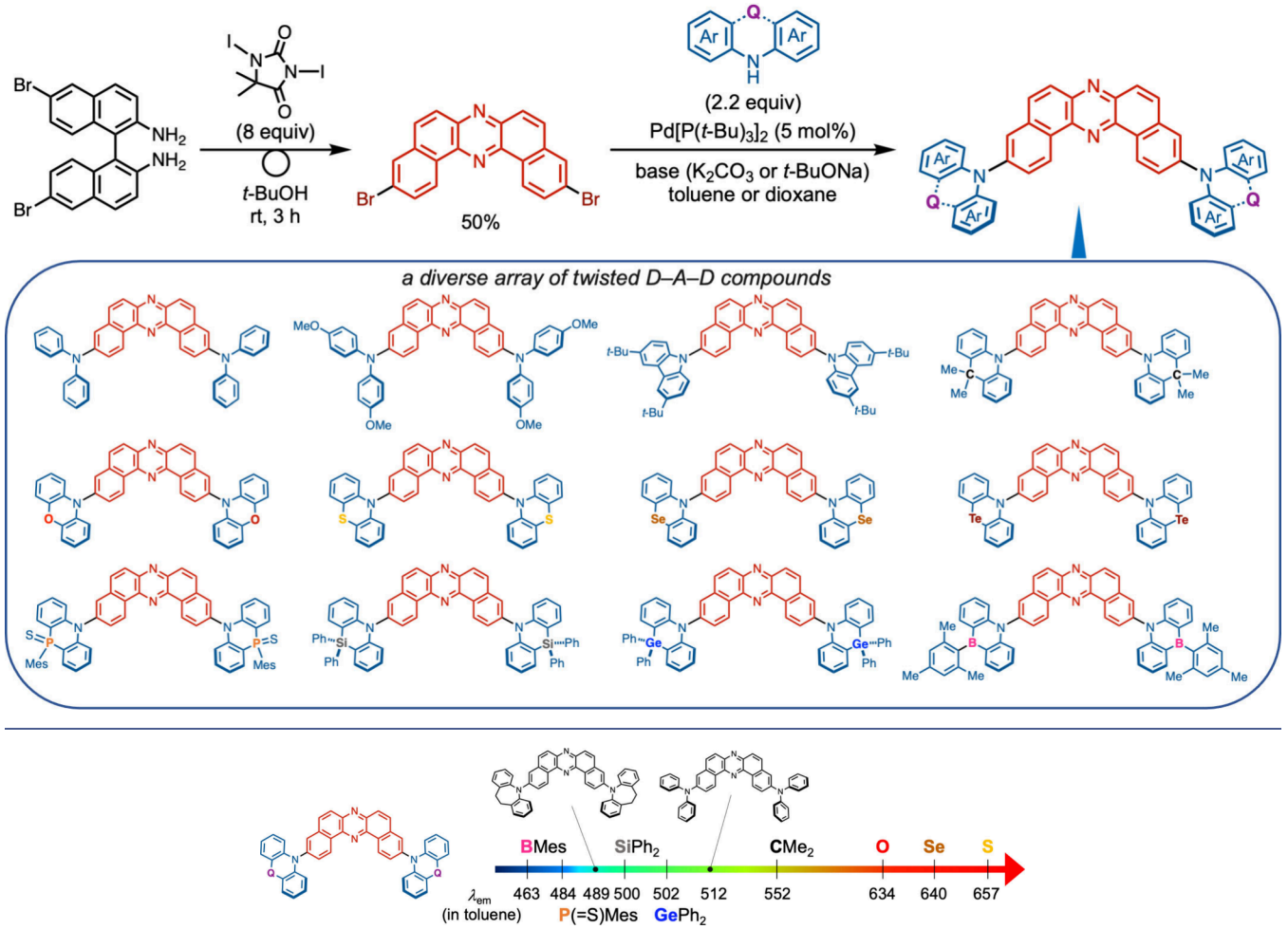

Figure 2. Relationship between the bridging unit (Q) in the donor and PL λ_{em} in toluene.

emitters. Additionally, we have investigated the modulation of emission properties of organic molecules by controlling the singlet−triplet energy gaps of the excited state through twisting or cyclizing the emitters and by controlling the excited-state energy via the generation of metastable states in the emitters.

In this Account, a summary of our accomplishments in modulating photofunctional properties through the effects of heteroatoms, conformation, and molecular topology is presented, employing our original U-shaped DBPHZ-cored D−A−D and D−A−D−A molecular scaffolds. Despite the close interrelation between conformational isomerism and molecular topology, this Account delineates conformers as three-dimensional spatial configurations of molecules, whereas molecular topology pertains to the connectivity of organic fragments (e.g., macrocyclic or linear connectivity). Discussions on the synthesis of other types of azaaromatics from 1,1′-binaphthalene-2,2′-diamines[21] and the investigations into the on-surface self-assembly of DBPHZ[22] and DBPHZ-based polymeric materials[23] are beyond the scope of this Account and are thus not included.

Synthesis of Twisted D−A−D Compounds

A general synthetic route to twisted D−A−D compounds is illustrated in Scheme 2. The pivotal and original electron-accepting building block, 3,11-dibromo-dibenzo[*a*,*j*]phenazine, is readily synthesized through an oxidative skeletal rearrangement of 6,6′-dibromo-binaphthalenediamine.[19] This dibromo compound serves as a valuable electrophilic coupling partner in a Pd-catalyzed Buchwald−Hartwig amination, yielding a diverse array of twisted D−A−D π-conjugated compounds in high yield.

Correlation between Heteroatom Substitution and Photoluminescence Wavelength

An important feature of the D−A−D scaffold is that the emission color in solution can be tuned within the visible light region by modulating the electron-donating power of the bridging unit (Q) in the donor. Figure 2 illustrates the correlation between the photoluminescence (PL) wavelength (λ_{em}) in toluene and the incorporated bridging unit.[1,2,4,24−28] When compared to a D−A−D compound with non-bridged donors (diphenylamine), incorporating divalent chalcogen atoms (O, S, Se) into the donor unit results in a significant red shift in PL of over 100 nm. These divalent chalcogen atoms possess lone pairs of electrons that can be donated into the π-electronic system, increasing the electron density of the donor units and facilitating charge separation (D^+-A^-) in the excited state, which is further stabilized by the twisted D−A−D scaffold (i.e., twisted intramolecular charge transfer).

In contrast to the divalent chalcogen atom-embedded D−A−D compounds, incorporating electropositive tetravalent group 14 element (χ_p Si: 1.90; Ge: 2.01) and the electron-deficient trivalent boron (χ_p 2.04) shifts the λ_{em} to the blue region

https://doi.org/10.1021/acs.accounts.4c00353
Acc. Chem. Res. 2024, 57, 2219−2232

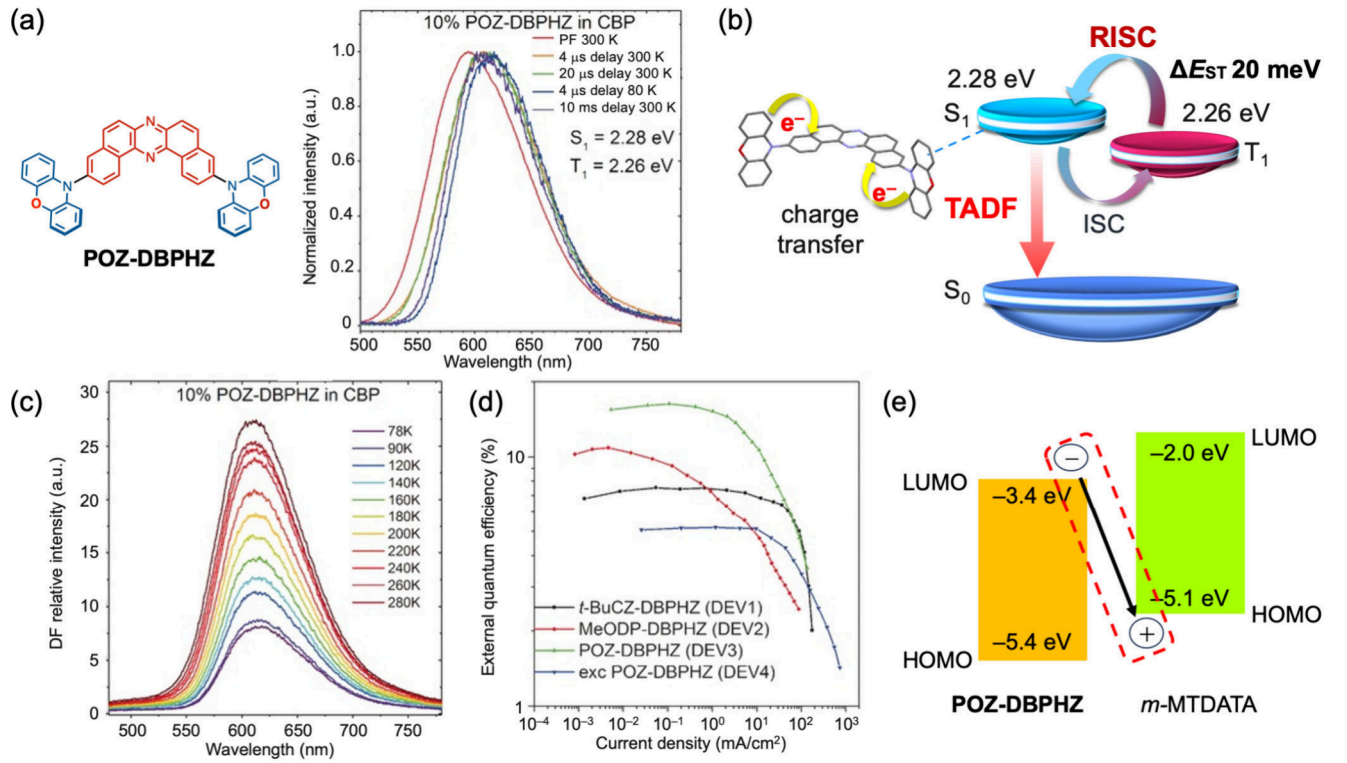

Figure 3. (a) Chemical structure of POZ-DBPHZ and its time-resolved PL spectra in CBP. (b) Illustrative TADF mechanism of POZ-DBPHZ in CBP. (c) Temperature-dependent PL spectra of POZ-DBPHZ in CBP. (d) EQE−current density characteristics of OLED devices. (e) Energy diagram of POZ-DBPHZ and *m*-MTDATA. Adapted with permission from ref 1. Copyright 2016 Wiley-VCH Verlag GmbH.

compared to the heteroatom-free D−A−D compound, due to the destabilization of the charge-transfer (CT) excited states. Coincidentally, the pentavalent phosphorus unit (Mes−P═S, where Mes represents 2,4,6-$Me_3C_6H_2$) serves as an electron-withdrawing group, probably due to the presence of a low-lying P−C or P−S σ^* bond. Also, the resonance structure contribution of the phosphonium form (Mes−P^+−S^-) can give us an intrinsic picture of the electron-deficient effect. Generally, there is a strong correlation between the electron-donating ability of the incorporated unit (Q) and λ_{em} in solution (Figure 2).

However, we observed that the true power of incorporating a bridging unit (Q) into the donor extends beyond merely modulating excited-state energy; it also introduces diversity into molecular conformation. For example, bridging diphenyl units of the donor with one carbon (CMe_2) or two carbons (CH_2CH_2) results in a significantly different λ_{em} (512 and 489 nm, respectively), despite the negligible difference in the electron-donating power of the bridging units. This variation reflects the dihedral angle between the donor and acceptor units, which strongly affects the conjugation length in both the ground and excited state. For instance, theoretical calculations suggest that the D−A−D molecule with single carbon-bridged donors (Q= CMe_2) predominantly adopts a conformation with a highly twisted D−A dihedral angle, whereas the D−A−D molecule with two carbon-bridged donors (CH_2CH_2) adopts a planar (axial-type) conformer. A highly twisted D−A−D structure results in a spatially separated HOMO/LUMO distribution, stabilizing the twisted intramolecular charge transfer excited state. Conversely, the planar D−A−D molecular conformation leads to significant overlap of HOMO and LUMO, facilitating a $\pi-\pi^*$ transition. The difference in the excited-state character accounts for the variation in the experimentally observed emission wavelengths (Figure 2). The details of these effects of conformation arising from the bridging unit (Q) will be discussed in the following sections.

Enhancing CT Character for Efficient TADF Manifestation

One of the key photophysical characteristics of the D−A−D compounds we developed is that T_1 is localized on the acceptor unit at approximately 2.40 eV, and this state is significantly less affected by external polarity than the CT state. Given that the S_1 of the D−A−D scaffold predominantly exhibits CT characteristics rather than locally excited (LE) characteristics in moderate to polar media, ΔE_{ST} can be readily adjusted by tuning the singlet CT energy to align with the energy level of the triplet excited state localized on the acceptor. A representative example demonstrating the tunability of ΔE_{ST} is the D−A−D compound with an oxygen-bridged donor (phenoxazine) (POZ-DBPHZ, Figure 3a).[1] POZ-DBPHZ displayed a very narrow ΔE_{ST} (20 meV) in 4,4′-bis(*N*-carbazolyl)-1,1′-biphenyl (CBP) matrix (Figure 3a).[1] In addition, the almost orthogonal orientation of the donor and acceptor units enables a spin-orbit charge transfer mechanism (Figure 3b). Notably, this is the first example of a spin-orbit charge transfer TADF coupled with the localized T_1 state of the acceptor. Thermal activation of TADF was clearly observed in the same host matrix (Figure 3c). The activation energy for TADF was determined to be 19 meV, which is consistent with the ΔE_{ST} value.

An intriguing aspect of the molecular design involves the number of donor units required to facilitate TADF. When one donor in POZ-DBPHZ was removed (resulting in a D−A type molecule), the ΔE_{ST} increased (110 meV in CBP), thereby reducing the TADF efficiency compared to POZ-DBPHZ.[29] While it might be assumed that a single D−A unit is sufficient to

https://doi.org/10.1021/acs.accounts.4c00353
Acc. Chem. Res. 2024, 57, 2219−2232

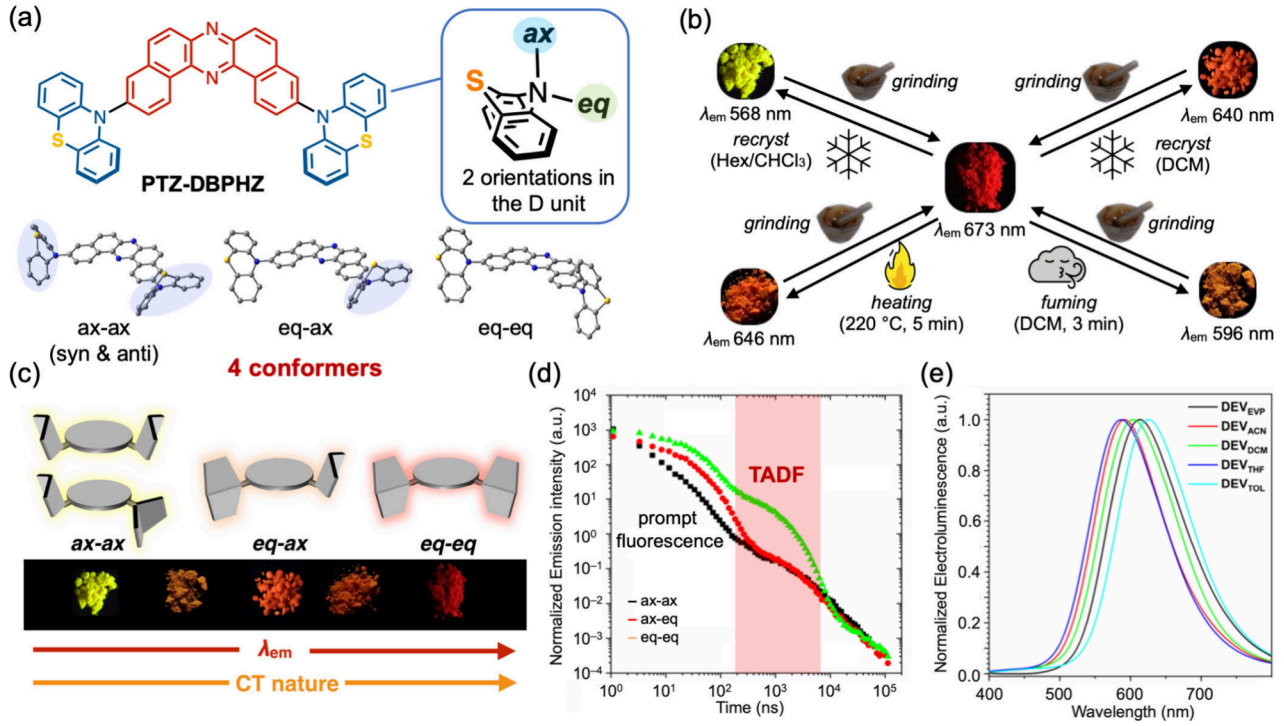

Figure 4. (a) Chemical structure and conformations of PTZ-DBPHZ. (b) Illustrative summary of external-stimuli responsiveness of PTZ-DBPHZ. Reproduced from ref 21. Available under a CC-BY NC license. Copyright 2020 Royal Society of Chemistry. (c) Correlation between conformation and emission color. Reproduced from ref 2. Available under a CC-BY license. Copyright 2017 Royal Society of Chemistry. (d) Time-resolved emission profiles of each conformer-enriched solid. (e) Electroluminescence spectra of solution-processed OLED devices fabricated with PTZ-DBPHZ from different organic solvents. Adapted from ref 34. Copyright 2019 Royal Society of Chemistry.

manifest TADF through intramolecular charge transfer, this result suggests that the presence of two donor units enhances the CT character in the excited state and minimizes ΔE_{ST}. This finding suggests that increasing the number of donor or acceptor units in a molecule is an effective strategy for enhancing the TADF performance. POZ-DBPHZ also exhibited excellent electrochemical reversibility and thermal stability (5 wt % decomposition temperature: 453 °C), enabling the fabrication of an OLED device by thermal deposition. The external quantum efficiency (EQE) of the device (DEV 3, Figure 3d) reached a very high value (16%) for orange TADF-OLED. Further optimization of device configurations by adding a hole injection layer (2,3,6,7,10,11-hexacyano-1,4,5,8,9,12-hexaazatriphenylene: HAT-CN) and removing an extra electron-transporting layer (2,9-dimethyl-4,7-diphenyl-1,10-phenanthroline: BCP) achieved an EQE close to the theoretical maximum (20.5%).[30]

The appropriate choice of a host matrix [4,4′,4′′-tris(*N*-3-methylphenyl-*N*-phenyl-amino)-triphenylamine: *m*-MTDATA] for the fabrication of an OLED-enabled near-infrared emission (λ_{em} 741 nm) from an exciplex between the emitter and the host material is noteworthy (Figure 3e). This represents one of the earliest examples of near-infrared TADF from a TADF exciplex.[31] By combining this orange-TADF emitter with blue and green TADF emitters, we achieved all-TADF warm-white OLED devices [*Commission International de l'Eclairage* (0.30, 0.40)−(0.33, 0.39) depending on voltage].[32]

External-Stimuli-Responsive Luminochromism via Conformational Interconversion

In 2017, we discovered that replacing the oxygen atom in POZ-DBPHZ with a sulfur atom resulted in a significant alternation in external-stimuli responsiveness (Figure 4).[2] The sulfur atom has a much larger atom radius (1.00 Å)[33] compared to oxygen (0.60 Å),[33] and phenothiazine (PTZ) consists of a 16 π-electron system (anti-aromatic if planar). Due to these factors, PTZ adopts a boat structure, presenting two possible orientations for a substituent on the nitrogen atom (equatorial: eq; axial: ax, Figure 4a). As a result, PTZ-DBPHZ can exist in four conformers [ax-ax (*syn* and *anti*), eq-ax, and eq-eq], each with different twisting angles of the donor units relative to the acceptor unit, leading to variations in ground- and excited-state energies. In fact, quantum chemical calculations suggest that the eq-eq-type conformer exhibits spatial separation of the HOMO and LUMO, which are located on the donor and acceptor units, respectively, due to the disconnection between these units. Conversely, the ax-ax-type conformer displays delocalized HOMO and LUMO over the π-conjugated skeleton, typical of planar or slightly twisted conjugated systems. This results in distinctly different absorption and photoluminescence properties, arising from the differences in the HOMO−LUMO energy gap and excited-state character (CT vs $\pi-\pi^*$).

We hypothesized that if the dominant conformer in the solid state could be regulated by external stimuli, then it would be possible to modulate emission properties by applying stimuli such as mechanical force and heat. This hypothesis was confirmed as the emission color of PTZ-DBPHZ changed significantly across multiple colors in response to various stimuli, such as grinding, heating, and exposure to organic solvent vapor (Figure 4b). Demonstrating conformational flexibility, X-ray crystallographic analysis of a single crystal grown from CH_2Cl_2 revealed a mixture of donor orientations (eq-ax). Most importantly, D−A−D compounds with carbon-bridged donors (dihydroacridine), bridging-atom-free donors (diphenylamine),

https://doi.org/10.1021/acs.accounts.4c00353
Acc. Chem. Res. 2024, 57, 2219−2232

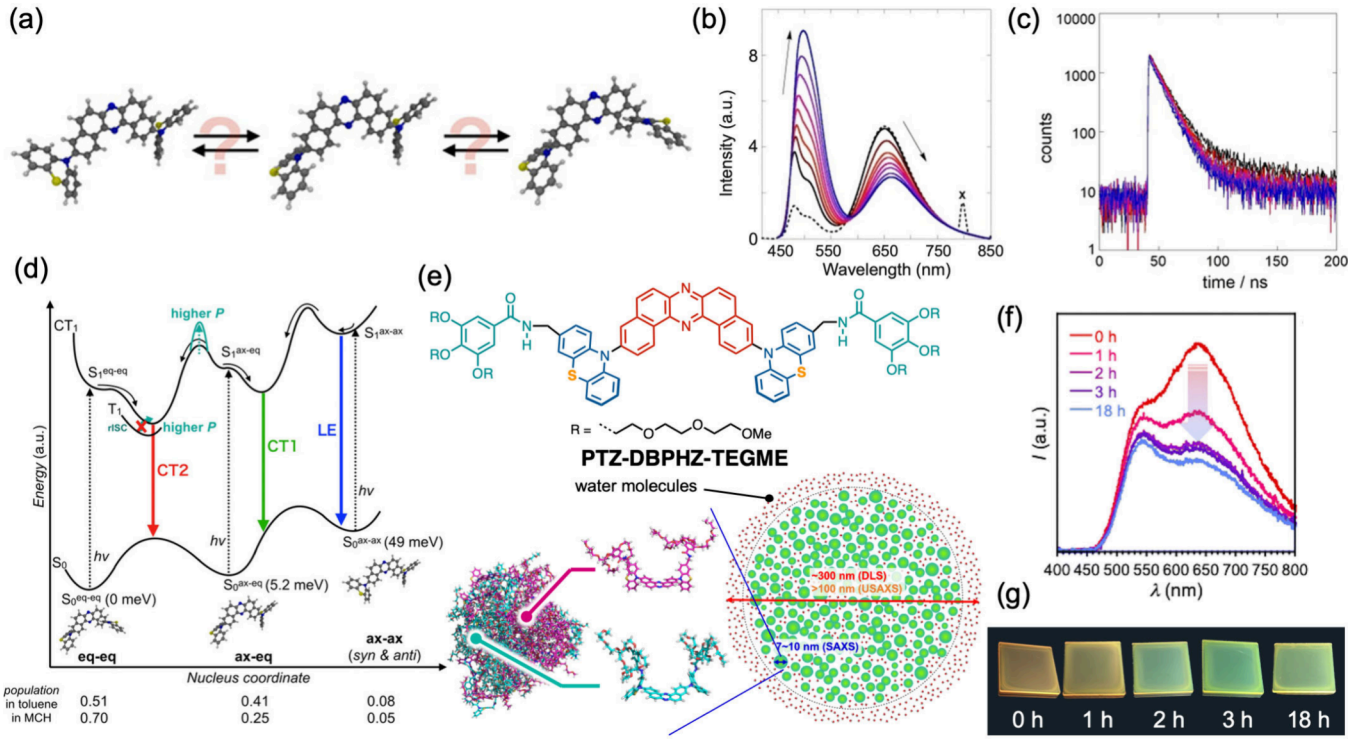

Figure 5. (a) Conformational interconversion of PTZ-DBPHZ in solution. (b) PL spectra and (c) PL decay of PTZ-DBPHZ in toluene as a function of hydrostatic pressure. (d) Illustrative energy diagram of conformers of PTZ-DBPHZ in the ground and excited states. Adapted with permission from ref 35. Copyright 2019 Wiley-VCH Verlag GmbH. (e) Chemical structure of PTZ-DBPHZ-TEGME and illustrative hierarchical structure of aggregates formed in water. (f) PL spectra and (g) photographs taken under a UV lamp (λ_{ex} 365 nm) of PTZ-DBPHZ-TEGME in poly(vinyl alcohol) film (1 wt %) as a function of exposure time under a humid atmosphere (relative humidity 75%). Adapted from ref 36. Available under a CC-BY NC license. Copyright 2024 Royal Society of Chemistry.

and an oxygen-bridged donor (POZ) did not exhibit significant external stimuli responsiveness. This clearly highlights the important role of the S atom in the donor unit in controlling conformation: a longer C−S bond than C−C/C−O single bonds allows for flexible orientation of the acceptor unit on the boat heterocyclic ring (eq or ax) and for locking the orientation as a metastable state at the same time. As the population of the equatorial orientation increases, the twisted intramolecular charge-transfer excited state is further stabilized, shifting the emission wavelength to the red region (Figure 4c). This correlation was also validated through time-resolved PL analysis of solids, where red-emitting solids displayed distinct TADF, while yellow-emitting solids predominantly exhibited prompt fluorescence (Figure 4d).[34] Notably, PTZ-DBPHZ represents the first example of a TADF-active, multicolor-changing mechanochromic organic material. The OLED fabricated with PTZ-DBPHZ achieved a comparable EQE (16.8%) to the POZ-DBPHZ-based OLED. Utilizing the conformer-dependent emission of PTZ-DBPHZ, we demonstrated that the electroluminescence color of solution-processable OLEDs could be readily modulated by changing the organic solvent used in the fabrication process (Figure 4e).[34]

Generally, the conformational flexibility of organic molecules is greater in solutions than in solid states. This raises a fundamental question: "Is it possible to regulate molecular conformation by applying external pressure in solution?" (Figure 5a). Spectroscopic analysis of PTZ-DBPHZ in solution under hydrostatic pressure provided an answer to this question.[35] Applying hydrostatic pressure (0.1−350 MPa) to a toluene solution of PTZ-DBPHZ resulted in a ratiometric change in the PL spectra (Figure 5b). The energetically lowest emission (CT emission from eq-eq) at around 650 nm decreased, while the energetically higher emissions at around 460 and 500 nm (LE and CT from ax-ax and ax-eq, respectively) increased as a function of hydrostatic pressure. Coincidentally, TADF was suppressed as a function of hydrostatic pressure (Figure 5c). These results indicate that the equilibrium among excited-state conformers can be regulated in solution through pressurization (Figure 5d). Elevating hydrostatic pressure increases the viscosity of the solvent (0.56−3.68 mPa·s), thereby suppressing molecular vibrations and rotations of the donor or acceptor units around the D−A connecting bonds, leading to a reduced TADF contribution.

Water presents a unique environment for hydrophobic organic molecules, where the entropy of water molecules is maximized and the contact area between water and hydrophobic organic molecules is minimized. Introducing six amphiphilic triethylene glycol monomethyl ether (TEGME) chains at the periphery of PTZ-DBPHZ enabled the molecule (PTZ-DBPHZ-TEGME, Figure 5e) to manifest high dispersibility in water.[36] In water, the molecule forms aggregates with hierarchical structures (Figure 5e), where small subunits of several nm size formed from molecules assemble in a larger aggregate particle (>100 nm). In the subunit (green particles in Figure 5e), a mixture of different conformers exists. Notably, poly(vinyl alcohol) films containing PTZ-DBPHZ-TEGME displayed two PL maxima corresponding to emissions from eq-eq and ax-ax and showed a ratiometric response to humidity (Figure 5f). This indicates that the CT excited state in the lower-energy region (>700 nm) is more readily quenched by water

https://doi.org/10.1021/acs.accounts.4c00353
Acc. Chem. Res. 2024, 57, 2219−2232

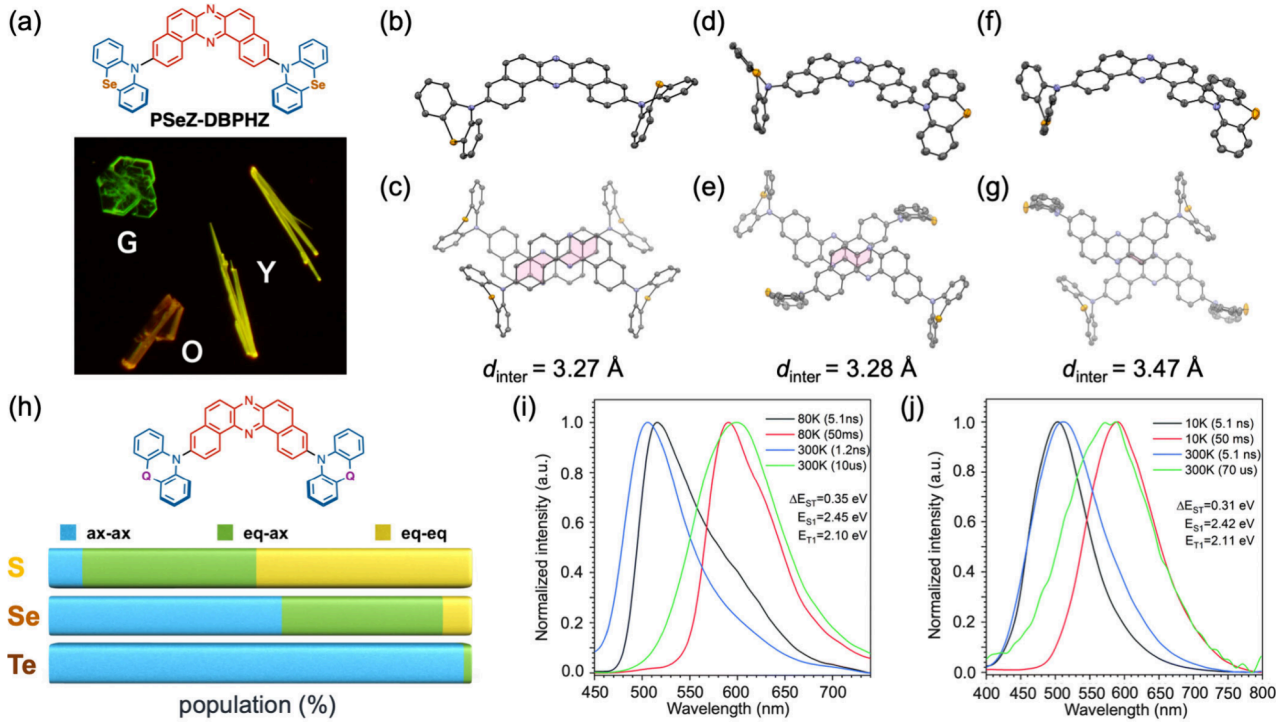

Figure 6. (a) Chemical structure of PSeZ-DBPHZ and photographs of its polymorphs (G, Y, and O) taken under the irradiation of a UV lamp (λ_{ex} = 365 nm). Molecular geometry in (b) G, (d) Y, and (f) O. Dimeric structure in (c) G, (e) Y, and (g) O. (h) Calculated population of conformers of D−A−D compounds in vacuum at 300 K. Time-resolved PL spectra of (i) PSeZ-DBPHZ and (j) PTeZ-DBPHZ in CBP. Adapted from ref 28. Copyright 2021 Royal Society of Chemistry.

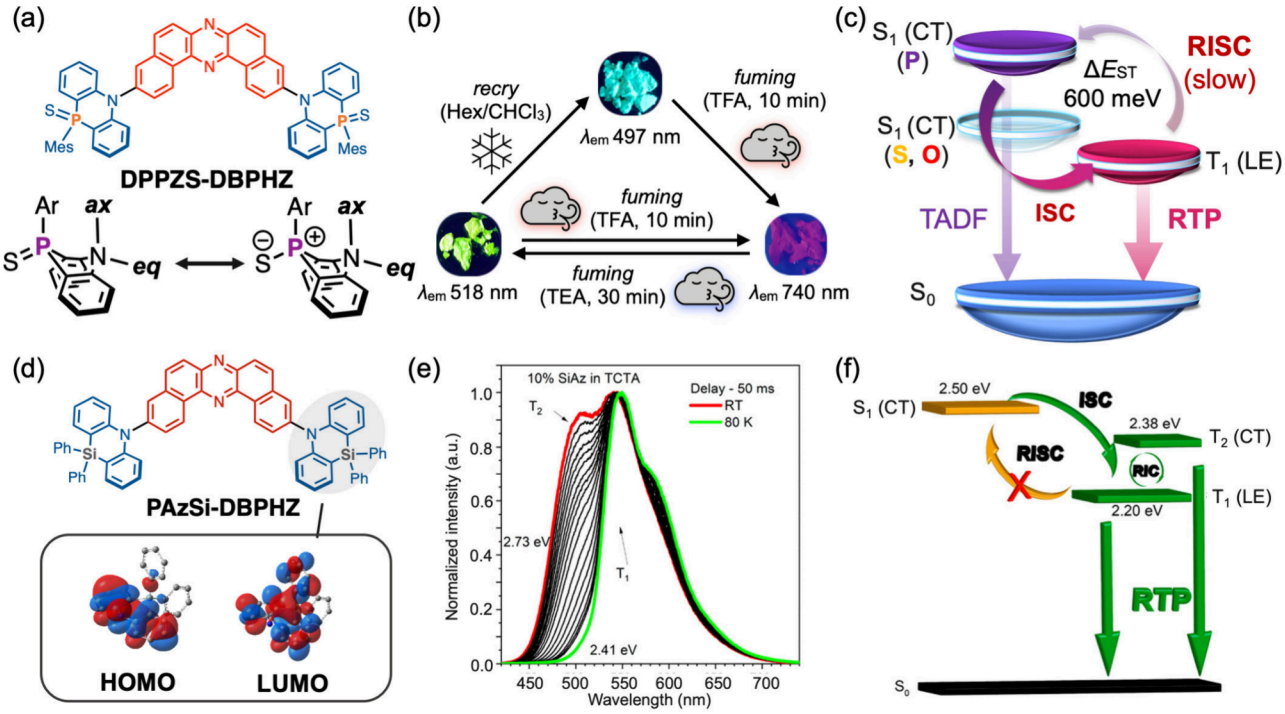

Figure 7. (a) Chemical structure of DPPZS-DBPHZ and resonance structures of the donor. (b) Illustrative summary of external-stimuli responsiveness of DPPZS-DBPHZ. Reproduced from ref 21. Available under a CC-BY NC license. Copyright 2020 Royal Society of Chemistry. (c) Proposed mechanism of dual emission of TADF and RTP from DPPZS-DBPHZ in Zeonex. (d) Chemical structure of PAzSi-DBPHZ and the frontier molecular orbitals of the donor. (e) Temperature-dependent PL spectra of PAzSi-DBPHZ in TCTA. (f) Proposed mechanism of dual-RTP in the TCTA. Adapted from ref 25. Copyright 2021 American Chemical Society.

through energy transfer to the vibrational levels of water than the LE excited state.[37] This ratiometric characteristic allows for the visualization of humidity through changes in emission color visible to the naked eye (Figure 5g). Additionally, as a related

https://doi.org/10.1021/acs.accounts.4c00353
Acc. Chem. Res. 2024, 57, 2219−2232

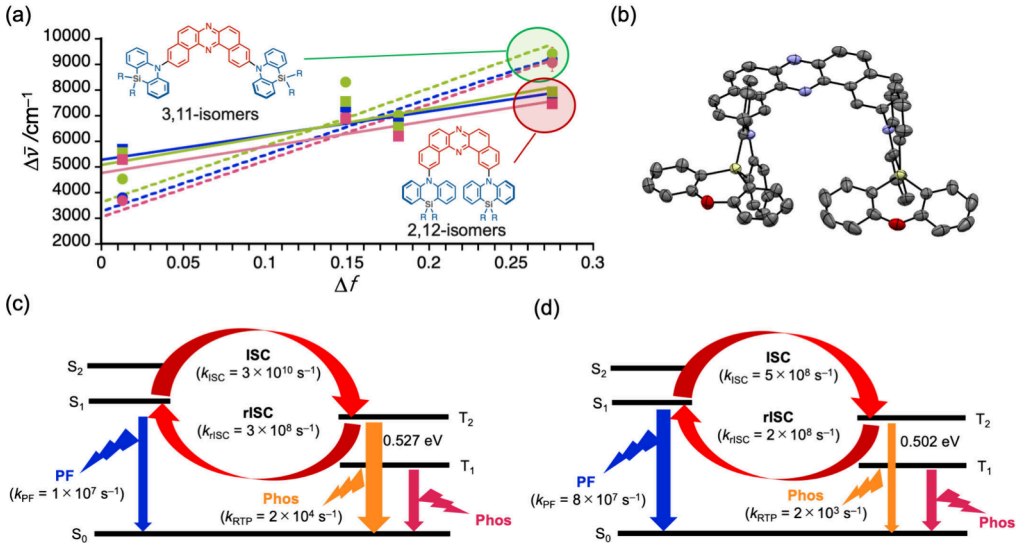

Figure 8. (a) Lippert−Mataga plots of 3,11-isomers and 2,12-isomers of PAzSi-DBPHZ (SiR_2 = $SiPh_2$, $Si(i\text{-}Pr)_2$ and dibenzo[*b*,*e*][1,4]oxasiline). Δf indicates the orientation polarizability of solvent, and $\Delta\bar{\nu}$ indicates the Stokes shift in wavenumber. (b) ORTEP of a 2,12-isomer. Theoretically calculated transition rates of photophysical processes of a (c) 3,11-isomer and (d) 2,12-isomer of PAzSi-DBPHZ. Adapted from ref 46. Copyright 2022 Royal Society of Chemistry.

humidity-responsive colorimetric function based on the DBPHZ D−A−D scaffold, the introduction of dendritic carbazole units, which possess greater structural flexibility than POZ and PTZ, enabled a reversible colorimetric response to humidity (relative humidity 3.9−84.3%) in a self-assembled solid.[38]

Modulation of Conformer-Specific Emissions through the Incorporation of Heavy Chalcogen Elements

Substitution of the S atom in PTZ-DBPHZ with its heavier congeners (Se and Te) enables the modulation of photophysical properties in a distinct manner.[28] Recrystallization of the selenium analogue of PTZ-DBPHZ (PSeZ-DBPHZ) from *n*-hexane/ethyl acetate produced three polymorphs (G, Y, and O), each exhibiting different PL colors: green, yellow, and orange, respectively (Figure 6a). Remarkably, these polymorphic single crystals demonstrated not only varying conformers (Figure 6b, d, and f) but also distinct stacking modes (Figure 6c, e, and g). This observation indicates that both the conformation and the extent of π-unit overlap significantly influence the excited-state energies.

Quantum chemical calculations elucidated the impact of incorporating heavier chalcogen atoms on conformational preferences: with an increase in atomic number, the ax-ax conformer becomes markedly more prevalent (Figure 6h). Energy decomposition analysis revealed that the repulsion between the lone pairs of N and Se/Te in the donor unit destabilizes the eq-type conformers relative to others, thereby enhancing the ax-ax preference. This shift in the dominant conformer facilitates dual emission from different conformers in solution, achieving single-molecule white PL, which is advantageous for designing single-molecular white emitters for lighting technology.[39] Moreover, the incorporation of Se and Te enabled the dual emission of prompt fluorescence and RTP in a CBP matrix, as evidenced by time-resolved PL spectra (Figure 6i and j). This phenomenon can be attributed to increased SOC resulting from the inherently large SOC constants of Se and Te. Theoretical calculations demonstrated that the SOC matrix element between the singlet ground state (S_0) and T_2 is larger (1.56 cm^{-1}) than that between S_0 and T_1 (1.32 cm^{-1}), and the T_1−T_2 energy gap ($\Delta E_{T_1-T_2}$ 400 meV) is smaller than that of ΔE_{ST} (490 meV). This finding suggests that RTP originates from the T_2 state, facilitated by thermally activated reverse interconversion (RIC) from T_1 to T_2.

Enhancement of Heavy Atom-Free RTP through the Incorporation of an Electropositive Bridging Unit in the Donor

The incorporation of an electropositive bridging unit into the donor enables RTP emission without the need for heavy-atom effects.[24,25] The integration of a phosphorus unit (Mes−P═S) into the donor structure results in conformational diversity due to the atomic radius similarity between phosphorus and sulfur (P: 1.00 Å vs. S: 1.00 Å)[33] (Figure 7a). As expected, the D−A−D compound with dihydrophenophosphazine sulfide (DPPZS) as the donor exhibited external-stimuli-responsive multicolor changes (Figure 7b). Compared to PTZ-DBPHZ, the amorphous solid-state emission wavelength of DPPZS-DBPHZ was observed in a significantly bluer region (λ_{em} = 534 nm, full width at half maximum = 2150 cm^{-1}). This shift in λ_{em} is attributed to the destabilization of the CT excited state (Figure 7c) due to the reduced electron-donating capability of the phosphorous center. Notably, DPPZS-DBPHZ embedded in a low-polar cyclic olefin polymer (Zeonex) displayed dual-delayed emission of TADF and RTP (Figure 7c), representing one of the earliest examples of concurrent dual-delayed emissions in solid films.[24] As previously mentioned, the T_1 state of the D−A−D system is generally localized on the DBPHZ core, and its energy level is less influenced by the polarity of the environment. Consequently, the destabilization of the S_1 state with CT character leads to an enlarged ΔE_{ST} (600 meV), which slows down the rate of RISC, thus making RTP and TADF compete (Figure 7c). These findings indicate that the fate of excited states can be modulated by the electron-donating ability of the donor unit in the D−A−D system, leading us to explore heavy atom-free RTP materials for organic electronics. While organometallic complex-based RTP emitters for OLEDs have been widely utilized,[40,41] they often contain heavy rare

https://doi.org/10.1021/acs.accounts.4c00353
Acc. Chem. Res. 2024, 57, 2219−2232

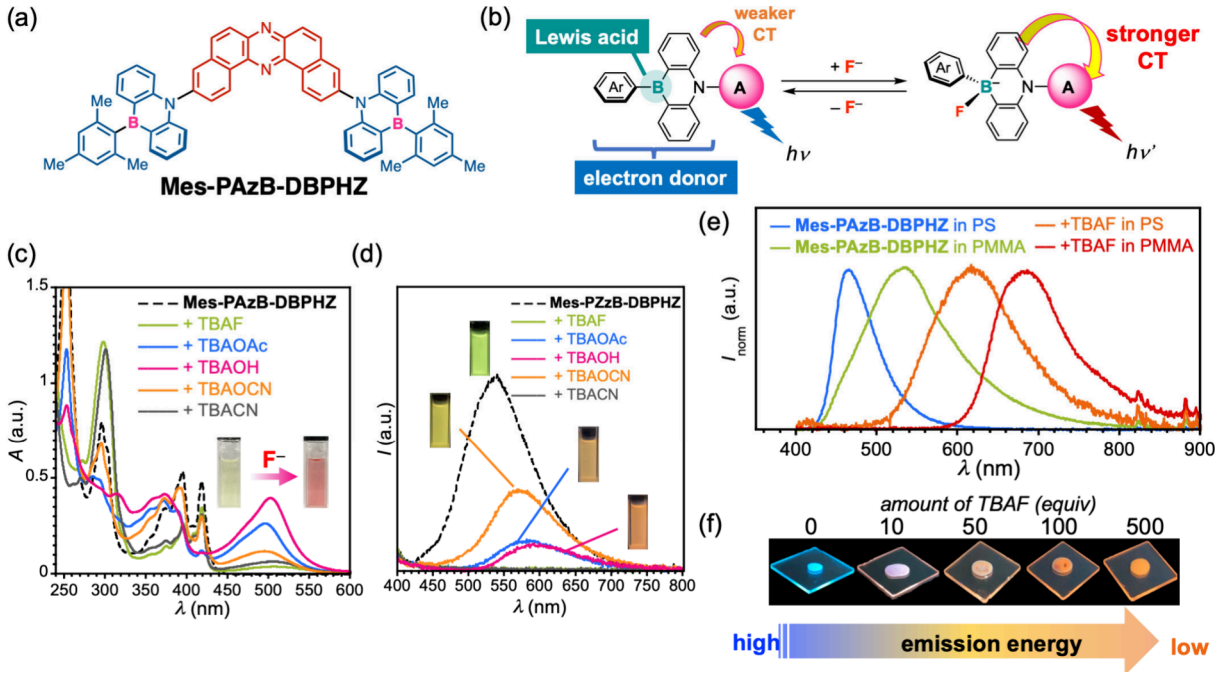

Figure 9. (a) Chemical structure of Mes-PAzB-DBPHZ. (b) Concept of the anion-responsive red shift in absorption and emission based on the PAzB structure. (c) UV−vis absorption and (d) PL spectra of Mes-PAzB-DBPHZ in the absence and presence of an anion in THF. The inset photographs in (c) were taken under visible light before and after the addition of fluoride, while the ones in (d) were taken under a UV lamp (λ_{ex} 365 nm) after the addition of anion. (e) PL spectra of Mes-PAzB-DBPHZ in polystyrene (PS) and poly(methyl methacrylate) (PMMA) in the absence and presence of tetrabutylammonium fluoride (TBAF). (f) Photographs of Mes-PAzB-DBPHZ with varied TBAF amounts in PS films taken under a UV lamp (λ_{ex} = 365 nm). Adapted from ref 4. Available under a CC-BY license. Copyright 2024 Wiley-VCH Verlag GmbH.

metals, raising concerns about production cost and resource depletion in the future. Therefore, developing heavy atom-free RTP materials from naturally abundant elements is an urgent research challenge. Despite pioneering research on heavy atom-free RTP emitters in OLEDs,[42−45] the EQE of these devices remains very low (<1%), primarily due to the quenching of long-lived triplet excitons through processes such as triplet−triplet annihilation and thermal non-radiative pathways.

To address the issue on low EQE of purely organic RTP materials, we designed a new D−A−D molecule by incorporating an electropositive element (Si) as the bridging atom in the donor (Figure 7d).[25] As evident from the frontier molecular orbitals of the donor (phenazasiline: PAzSi), effective (C−Si)$\sigma-\pi$ and (C−Si)$\sigma^*-\pi^*$ hyperconjugation lowers the HOMO/LUMO energy levels. Notably, the D−A−D compound (PAzSi-DBPHZ) exhibited dual-RTP at approximately λ_{em} 500 and 550 nm in a 4,4′,4-tris(carbazol-9-yl)-triphenylamine (TCTA) matrix, where the intensity of the shorter-wavelength emission (500 nm) is thermally activated (Figure 7e). At a glance, this thermally activated behavior appeared to be a TADF process. However, a closer examination of the time-resolved photophysics revealed that the S_1 energy (2.50 eV) differed from the triplet states (2.38 and 2.20 eV), and the lifetime of the delayed emission was in the millisecond range (τ_1 44.7 ms; τ_2 1.62 ms). Based on these results, we propose that the dual RTP originates from T_1 and T_2, both of which are lower in energy than S_1 (Figure 7f). Since $\Delta E_{T_1-T_2}$ (180 meV) is smaller than ΔE_{ST} (300 meV), the RIC process is more efficiently activated than RISC, yielding dual RTP. Quantum chemical calculations also support this mechanism: T_1 has LE character, while T_2 has CT character, and thus the SOC matrix element for the T_2-S_0 transition is much larger (5.85 cm^{-1}) than for the T_1-S_0 transition (0.87 cm^{-1}). The faster radiative deactivation (RTP) from the T_2 and the RIC process should consume long-lived triplet excitons, thereby displaying efficient RTP. Indeed, the OLED fabricated with PAzSi-DBPHZ emitter achieved a very high EQE of up to 4.1%, which is among the highest reported for heavy atom-free RTP material-based devices.

Modulation of Photophysical Properties through Regioisomerism

Regioisomerism significantly influences the photophysical behavior of the D−A−D scaffold.[46] We synthesized a series of 3,11- and 2,12-disubstituted PAzSi-DBPHZ compounds with various substituents on the Si center. The Lippert−Mataga plots revealed that the slope and intercept of the regression lines differed substantially (Figure 8a). The larger slopes for 3,11-isomers, compared to 2,12-isomers, indicated greater changes in the dipole moment from the S_0 to the excited state, attributable to the larger contribution of the CT state in the excited state for 3,11-isomers. Conversely, the larger intercepts for 2,12-isomers suggested more significant structural changes in the excited state for these isomers. These unique characteristics were further corroborated by theoretical calculations: the eq-ax conformer is more stable in the excited state for 2,11-isomers, while the eq-eq conformer is more stable in the ground state (Figure 8b). Consequently, the photophysical outcomes of the regioisomers are highly dependent on their conformational preferences in the excited and ground states, leading to a combination of TADF and RTP (Figure 8c and d). Through the studies, we successfully identified a highly efficient heavy atom-free RTP emitter [3,11-isomer of PAzSi-DBPHZ, SiR_2 = Si(*i*-Pr)$_2$] for OLEDs, achieving an EQE of as high as 7.4%.

https://doi.org/10.1021/acs.accounts.4c00353
Acc. Chem. Res. 2024, 57, 2219−2232

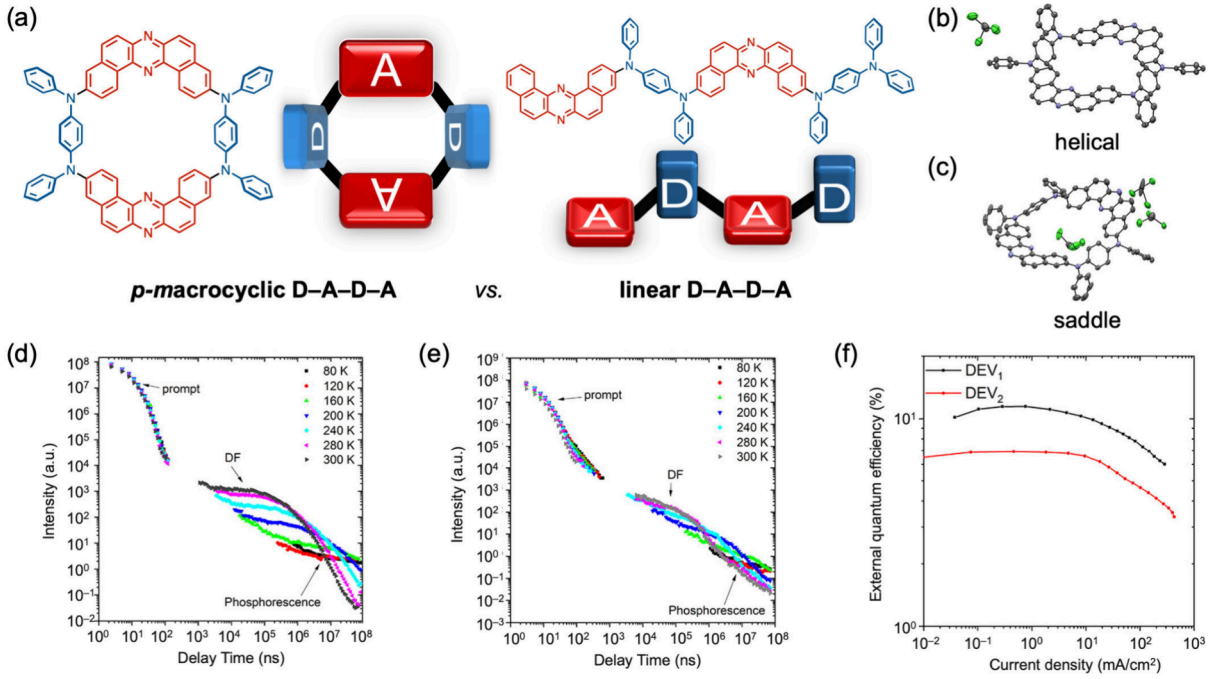

Figure 10. (a) Chemical structures of *p*-macrocyclic D−A−D−A and linear D−A−D−A. ORTEP of (b) helical and (c) saddle conformers of *p*-macrocyclic D−A−D−A. Time-resolved PL intensity of (d) *p*-macrocyclic D−A−D−A and (e) linear D−A−D−A in CBP. (f) EQE-current-density characteristics of the OLED devices fabricated with *p*-macrocyclic D−A−D−A (DEV_1) and linear D−A−D−A (DEV_2). Adapted from ref 3. Copyright 2020 American Chemical Society.

Tuning Anion-Responsive Absorption and Emission by Balancing the Contradictory Roles of Donors

Incorporating a trivalent boron as the bridge in the D−A−D scaffold (Mes-PAzB-DBPHZ, Figure 9a) enables an unprecedented anion-responsive colorimetric and fluorometric red shift in both solution and solid states.[4] Colorimetric and fluorometric anion sensors based on triarylborane have been extensively developed, leveraging the Lewis acidic nature of the trivalent boron center and the photoactive properties arising from extended π-electron systems.[47−52] Nevertheless, most triarylborane-based anion sensors reported thus far exhibit a colorimetric and/or fluorometric blue shift or "turn-off" response to anions due to mechanisms involving the disruption of the π-conjugation or suppression of intramolecular CT upon anion coordination to the boron center. In contrast, strategies for manifesting anion-responsive red shifts in triarylborane-based sensors are scarce.

In 2024, we introduced a molecular design strategy to realize an anion-responsive red shift in absorption and emission by leveraging the dual roles of phenazaborine (PAzB, Figure 9b). When the PAzB is connected to a highly electron-deficient unit (acceptor A in Figure 9b), intramolecular CT occurs from the weak donor (PAzB) to the acceptor unit. Simultaneously, the trivalent boron center in the PAzB acts as a Lewis acid, capturing anions such as fluoride and hydroxide to form a tetracoordinate borate, which increases the electron density in the donor and enhances intramolecular CT, resulting in a red shift in absorption and emission (Figure 9b). As designed, Mes-PAzB-DBPHZ exhibited a significant red shift in absorption in THF, attributed to the intramolecular CT transition, from λ_{abs} 420 to 500 nm upon the addition of anions such as fluoride, acetate, and cyanide, leading to a color change from pale yellow to pink (Figure 9c). Concurrently, a red shift in the PL spectra was also observed for the same set of anions, resulting in a change in the emission color from green to orange (Figure 9d). Notably, this red-shift concept was effective even in the polymer matrix films (Figure 9e). By combining the polarity of the polymer matrix with the anion-triggered intramolecular CT enhancement, PL color was successfully modulated across the entire visible-light spectrum. The composition of the neutral triarylborane form and its borate was controlled by the amount of fluoride added, thus modulating the relative intensity of dual emission peaks (Figure 9f). Utilizing this modularity, warm white emission [*Commission International de l'Eclairage* (0.39, 0.33)] was achieved by balancing the dual emission (Figure 9f).

Modulation of Emission Properties through Molecular Topology

Molecular topology significantly impacts the photophysical properties. Utilizing the U-shaped structure of DBPHZ, we successfully synthesized a macrocyclic D−A−D−A compound (*p*-macrocyclic D−A−D−A, Figure 10a) and its linear analogue (linear D−A−D−A, Figure 10a) to examine the efficacy of cyclizing D−A repeating units.[3,53,54] The macrocyclic compound exhibited polymorphs arising from different conformers (helical and saddle, Figure 10b and c), which displayed distinct PL colors (λ_{em} = 594 and 654 nm, respectively). Although the PL emission in diluted solutions did not vary significantly, there was a notable difference in TADF behavior in a solid host (CBP) matrix. Time-resolved PL analysis revealed that the macrocyclic compound exhibited a much more pronounced TADF compared to the linear analogue (Figure 10d and e). Reflecting this difference in TADF behavior, the OLED device fabricated with the macrocyclic compound demonstrated a significantly higher EQE of 11.6% compared with 6.9% for the linear analogue (Figure 10f). These results clearly demonstrate the efficacy of cyclizing D−A repeating units to enhance TADF performance, likely due to the suppression of nonradiative pathways through the appropriate rigidification of molecular

https://doi.org/10.1021/acs.accounts.4c00353
Acc. Chem. Res. 2024, 57, 2219−2232

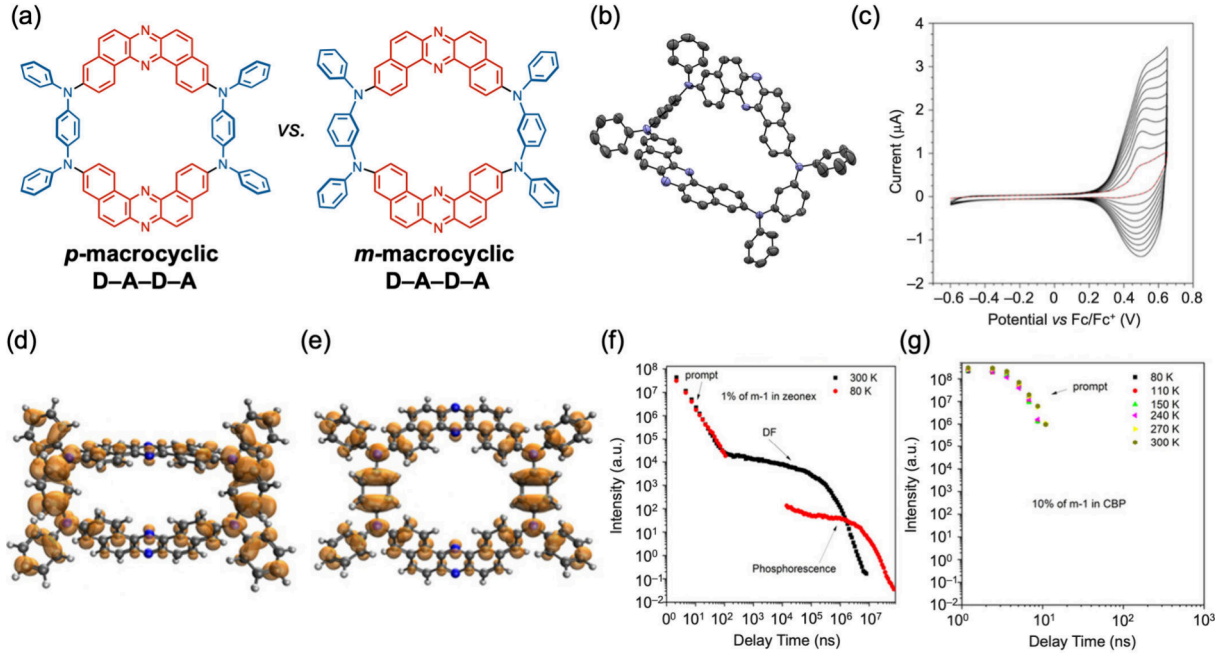

Figure 11. (a) Chemical structures of *p*- and *m*-macrocyclic D−A−D−A. (b) ORTEP of the *m*-macrocyclic D−A−D−A. (c) Sweep-repeated cyclic voltammograms of *m*-macrocyclic D−A−D−A. Spin density of diradical dications of (d) *m*- and (e) *p*-macrocyclic D−A−D−A. PL decay of *m*-macrocyclic D−A−D−A in (f) Zeonex and (g) CBP. Adapted with permission from ref 55. Copyright 2020 Wiley-VCH Verlag GmbH.

movement by the ring structure. Notably, this is the first example of a macrocyclic TADF emitter used in an OLED device.

Not only the cyclic structure but also the macrocyclic topology significantly affects physicochemical properties.[55] We synthesized a macrocyclic regioisomer comprising two DBPHZ acceptors and two *m*-phenylenediamine donors (*m*-macrocyclic D−A−D−A, Figure 11a) and compared its physicochemical properties with those of *p*-macrocyclic D−A−D−A. X-ray crystallographic analysis revealed that the *m*-linked macrocycle adopted a saddle-shaped conformation, and the interplane angle of the two DBPHZ panels was much smaller (91°) than that of the *p*-linked isomer (148°) (Figure 11b). Distinct differences in physicochemical properties emerged from the molecular topology, particularly in affecting the electrochemical behavior. While the *p*-macrocyclic D−A−D−A exhibited reversible redox behavior in cyclic voltammetry, the *m*-macrocyclic D−A−D−A showed an irreversible oxidation process due to oxidative polymerization on the electrode (Figure 11c). This difference was rationalized by examining the spin density distribution of the diradical dication of the macrocycles. In *p*-macrocyclic D−A−D−A, the spin density is localized across the entire macrocyclic system, whereas in *m*-macrocyclic D−A−D−A, the spin is localized at the ortho position of the *N*-phenyl units in the donor (Figure 11d and e). Consequently, electrochemical polymerization likely occurred at the ortho position. Notably, the macrocyclic topology also had a significant impact on the TADF performance. In solution, the TADF contribution of *m*-macrocyclic D−A−D−A was 10%, which was significantly lower than that of *p*-macrocyclic D−A−D−A (60%). Additionally, in solid matrices, TADF was very weak in Zeonex and almost disappeared in CBP (Figure 11f and g). These findings underscore the importance of carefully considering the molecular topology when designing TADF materials.

CONCLUSIONS AND OUTLOOK

In this Account, I summarize our contributions to modulating the photophysical properties of organic emitters using a twisted D−A−D system that comprises a U-shaped dibenzophenazine as the acceptor and bridged diarylamines as the donors. Based on our findings and discussions, several critical design principles for modulating the photophysical properties of D−A-type organic molecules can be derived as follows:

1. Incorporating heteroatomic units into an organic fragment is beneficial not only for adjusting their orbital energies but also for regulating their conformation. This approach can be employed to tune emission wavelengths and manifest specific photofunctions such as thermally activated delayed fluorescence, room-temperature phosphorescence, or both and others.
2. Generating conformational diversity that is interconvertible through heteroatomic incorporation is advantageous for designing stimuli-responsive organic materials. This design principle extends beyond mechanochromic luminescence materials, such as ours, to include themochromic, humidity-responsive materials and single-molecular bioprobes to explore various external stimuli.
3. The molecular topology created by fragment connectivity, beyond the typical linear structure, significantly impacts photophysical properties. For instance, macrocyclization with appropriate rigid π-conjugated linkers can enhance thermally activated delayed fluorescence by suppressing molecular rotation and vibration.

Although significant progress has been made, as discussed above, in designing organic emitters to modulate their photophysical properties, substantial challenges remain in utilizing the aforementioned design principles in future research. For instance, understanding the synergistic effects of incorporating two or more different heteroatoms into organic fragments on

https://doi.org/10.1021/acs.accounts.4c00353
Acc. Chem. Res. 2024, 57, 2219−2232

the control of molecular conformation warrants further exploration. This understanding would be instrumental for single-molecule control of photophysical properties and could enable high-resolution analysis of very weak (nano- to piconewton order) forces within biological tissue, such as a lipid membrane. Additionally, controlling the conformation on the substrate surface of electronic devices through the heteroatomic effect in a specific orientation could enhance the out-coupling efficiency of lighting devices. Moreover, incorporating more complex molecular topologies, such as molecular knots, links, and catenanes,[56] could lead to the development of high-performance chiroptical materials.

AUTHOR INFORMATION

Corresponding Author

Youhei Takeda − *Department of Applied Chemistry, Graduate School of Engineering, Osaka University, Suita, Osaka 565-0871, Japan;* orcid.org/0000-0001-9103-4238; Email: takeda@chem.eng.osaka-u.ac.jp

Complete contact information is available at: https://pubs.acs.org/10.1021/acs.accounts.4c00353

Notes

The author declares no competing financial interest.

Biography

Youhei Takeda completed his undergraduate education at Waseda University in 2005. After obtaining his Ph.D. from Kyoto University in 2010 under the supervision of Professor Tamejiro Hiyama, he pursued postdoctoral studies in the Timothy M. Swager group at Massachusetts Institute of Technology. During this term, he was appointed as a JSPS research fellow (DC2 and PD). He started his academic career as an assistant professor at Osaka University in 2011, and he was promoted to associate professor in 2015. Concurrently, he was appointed as an adjunct lecturer at Vietnam-Japan-University in 2015. His research interests include the design, synthesis, and interdisciplinary applications of heteroatom-embedded exotic π-conjugated organic molecules.

ACKNOWLEDGMENTS

The research works disclosed herein were supported by KAKENHI, Grant-in-Aid for Scientific Research on Innovative Areas (JP15H00997, JP17H05155, and JP19H05716), Grant-in-Aid for Scientific Research (B) (JP20H02813, JP23K26730, JP23H02037, and JP23H01852), and Grant-in-Aid for Challenging Research (Exploratory) (JP21K18960) from MEXT and Research Grants from Izumi Science and Technology Foundation, the Murata Science Foundation, the Asahi Glass Foundation, the Japan Science Society, the Japan Prize Foundation, Kansai Research Foundation for Technology Promotion, Iketani Science and Technology Foundation, the Mitsubishi Foundation, Japan Association for Chemical Innovation, and ENEOS TONENGENRAL Research/Development Encouragement & Scholarship Foundation.

REFERENCES

(1) Data, P.; Pander, P.; Okazaki, M.; Takeda, Y.; Minakata, S.; Monkman, A. P. Dibenzo[*a,j*]phenazine-Cored Donor-Acceptor-Donor Compounds as Green-to-Red/NIR Thermally Activated Delayed Fluorescence Organic Light Emitters. *Angew. Chem. Int. Ed.* **2016**, *55*, 5739−5744.

(2) Okazaki, M.; Takeda, Y.; Data, P.; Pander, P.; Higginbotham, H.; Monkman, A. P.; Minakata, S. Thermally Activated Delayed Fluorescent Phenothiazine-Dibenzo[*a,j*]phenazine-Phenothiazine Triads Exhibiting Tricolor-Changing Mechanochromic Luminescence. *Chem. Sci.* **2017**, *8*, 2677−2686.

(3) Izumi, S.; Higginbotham, H. F.; Nyga, A.; Stachelek, P.; Tohnai, N.; de Silva, P.; Data, P.; Takeda, Y.; Minakata, S. Thermally Activated Delayed Fluorescent Donor-Acceptor-Donor-Acceptor π-Conjugated Macrocycle for Organic Light-Emitting Diodes. *J. Am. Chem. Soc.* **2020**, *142*, 1482−1491.

(4) Aota, N.; Nakagawa, R.; de Sousa, L. E.; Tohnai, N.; Minakata, S.; de Silva, P.; Takeda, Y. Anion-Responsive Colorimetric and Fluorometric Red-Shift in Triarylborane Derivatives: Dual Role of Phenazaborine as Lewis Acid and Electron Donor. *Angew. Chem. Int. Ed.* **2024**, *63*, e202405158.

(5) Zhang, G.; Lin, F. R.; Qi, F.; Heumüller, T.; Distler, A.; Egelhaaf, H.-J.; Li, N.; Chow, P. C. Y.; Brabec, C. J.; Jen, A. K.-Y.; Yip, H.-L. Renewed Prospects for Organic Photovoltaics. *Chem. Rev.* **2022**, *122*, 14180−14274.

(6) Zhang, Y.; Wang, Y.; Gao, C.; Ni, Z.; Zhang, X.; Hu, W.; Dong, H. Recent Advances in N-Type and Ambipolar Organic Semiconductors and Their Multi-Functional Applications. *Chem. Soc. Rev.* **2023**, *52*, 1331−1381.

(7) Wang, L.; Zhu, W. Organic Donor-Acceptor Systems for Photocatalysis. *Adv. Sci.* **2024**, *11*, e2307227.

(8) Yang, Z.; Mao, Z.; Xie, Z.; Zhang, Y.; Liu, S.; Zhao, J.; Xu, J.; Chi, Z.; Aldred, M. P. Recent Advances in Organic Thermally Activated Delayed Fluorescence Materials. *Chem. Soc. Rev.* **2017**, *46*, 915−1016.

(9) Parker, C. A.; Hatchard, C. G. Triplet-Singlet Emission in Fluid Solutions. Phosphorescence of Eosin. *Trans. Faraday Soc.* **1961**, *57*, 1894−1904.

(10) Dias, F. B.; Penfold, T. J.; Monkman, A. P. Photophysics of Thermally Activated Delayed Fluorescence Molecules. *Methods Appl. Fluoresc.* **2017**, *5*, 012001.

(11) Eng, J.; Penfold, T. J. Open Questions on the Photophysics of Thermally Activated Delayed Fluorescence. *Commun. Chem.* **2021**, *4*, 91.

(12) Uoyama, H.; Goushi, K.; Shizu, K.; Nomura, H.; Adachi, C. Highly Efficient Organic Light-Emitting Diodes from Delayed Fluorescence. *Nature* **2012**, *492*, 234−238.

(13) Zhang, T.; Xiao, Y.; Wang, H.; Kong, S.; Huang, R.; Ka-Man Au, V.; Yu, T.; Huang, W. Highly Twisted Thermally Activated Delayed Fluorescence (TADF) Molecules and Their Applications in Organic Light-Emitting Diodes (OLEDs). *Angew. Chem. Int. Ed.* **2023**, *62*, e202301896.

(14) Caine, J. R.; Hu, P.; Gogoulis, A. T.; Hudson, Z. M. Unlocking New Applications for Thermally Activated Delayed Fluorescence Using Polymer Nanoparticles. *Acc. Mater. Res.* **2023**, *4*, 879−891.

(15) Mukherjee, S.; Thilagar, P. Recent Advances in Purely Organic Phosphorescent Materials. *Chem. Commun.* **2015**, *51*, 10988−11003.

(16) Hirata, S. Recent Advances in Materials with Room-Temperature Phosphorescence: Photophysics for Triplet Exciton Stabilization. *Adv. Opt. Mater.* **2017**, *5*, 1700116.

(17) Kenry; Chen, C.; Liu, B. Enhancing the Performance of Pure Organic Room-Temperature Phosphorescent Luminophores. *Nat. Commun.* **2019**, *10*, 2111.

(18) Data, P.; Takeda, Y. Recent Advancements in and the Future of Organic Emitters: TADF- and RTP-Active Multifunctional Organic Materials. *Chem.—Asian J.* **2019**, *14*, 1613−1636.

(19) Takeda, Y.; Okazaki, M.; Minakata, S. Oxidative Skeletal Rearrangement of 1,1′-Binaphthalene-2,2′-Diamines (BINAMs) via C-C Bond Cleavage and Nitrogen Migration: A Versatile Synthesis of U-Shaped Azaacenes. *Chem. Commun.* **2014**, *50*, 10291−10294.

(20) Thom, K. A.; Förster, T.; Weingart, O.; Goto, S.; Takeda, Y.; Minakata, S.; Gilch, P. The Photophysics of Dibenzo[*a,j*]phenazine. *ChemPhotoChem.* **2021**, *5*, 335−347.

(21) Takeda, Y.; Data, P.; Minakata, S. Alchemy of Donor-Acceptor-Donor Multi-Photofunctional Organic Materials: From Construction of Electron-Deficient Azaaromatics to Exploration of Functions. *Chem. Commun.* **2020**, *56*, 8884−8894.

(22) Kawai, S.; Kher-Elden, M. A.; Sadeghi, A.; Abd El-Fattah, Z. M.; Sun, K.; Izumi, S.; Minakata, S.; Takeda, Y.; Lobo-Checa, J. Near Fermi Superatom State Stabilized by Surface State Resonances in a Multiporous Molecular Network. *Nano Lett.* **2021**, *21*, 6456−6462.
(23) Izumi, S.; Inoue, K.; Nitta, Y.; Enjou, T.; Ami, T.; Oka, K.; Tohnai, N.; Minakata, S.; Fukushima, T.; Ishiwari, F.; Takeda, Y. 3,11-Diaminodibenzo[*a,j*]phenazine: Synthesis, Properties, and Applications to Tröger's Base-Forming Ladder Polymerization. *Chem.—Eur. J.* **2023**, *29*, e202202702.
(24) Takeda, Y.; Kaihara, T.; Okazaki, M.; Higginbotham, H.; Data, P.; Tohnai, N.; Minakata, S. Conformationally-Flexible and Moderately Electron-Donating Units-Installed D-A-D Triad Enabling Multicolor-Changing Mechanochromic Luminescence, TADF and Room-Temperature Phosphorescence. *Chem. Commun.* **2018**, *54*, 6847−6850.
(25) Higginbotham, H. F.; Okazaki, M.; de Silva, P.; Minakata, S.; Takeda, Y.; Data, P. Heavy-Atom-Free Room-Temperature Phosphorescent Organic Light-Emitting Diodes Enabled by Excited States Engineering. *ACS Appl. Mater. Interfaces* **2021**, *13*, 2899−2907.
(26) Nyga, A.; Kaihara, T.; Hosono, T.; Sipala, M.; Stachelek, P.; Tohnai, N.; Minakata, S.; de Sousa, L. E.; de Silva, P.; Data, P.; Takeda, Y. Dual-Photofunctional Organogermanium Compound Based on Donor-Acceptor-Donor Architecture. *Chem. Commun.* **2022**, *58*, 5889−5892.
(27) Zimmermann Crocomo, P.; Kaihara, T.; Kawaguchi, S.; Stachelek, P.; Minakata, S.; de Silva, P.; Data, P.; Takeda, Y. The Impact of C_2 Insertion into a Carbazole Donor on the Physicochemical Properties of Dibenzo[*a,j*]phenazine-Cored Donor-Acceptor-Donor Triads. *Chem.—Eur. J.* **2021**, *27*, 13390−13398.
(28) Goto, S.; Nitta, Y.; Decarli, N. O.; de Sousa, L. E.; Stachelek, P.; Tohnai, N.; Minakata, S.; de Silva, P.; Data, P.; Takeda, Y. Revealing the Internal Heavy Chalcogen Atom Effect on the Photophysics of the Dibenzo[*a,j*]phenazine-Cored Donor-acceptor-donor Triad. *J. Mater. Chem. C* **2021**, *9*, 13942−13953.
(29) Izumi, S.; Govindharaj, P.; Drewniak, A.; Crocomo, P. Z.; Minakata, S.; de Sousa, L. E.; de Silva, P.; Data, P.; Takeda, Y. Comparative Study of Thermally Activated Delayed Fluorescent Properties of Donor-Acceptor and Donor-Acceptor-Donor Architectures Based on Phenoxazine and Dibenzo[*a,j*]phenazine. *Beilstein J. Org. Chem.* **2022**, *18*, 459−468.
(30) Zimmermann Crocomo, P.; Okazaki, M.; Hosono, T.; Minakata, S.; Takeda, Y.; Data, P. Dibenzophenazine-Based TADF Emitters as Dual Electrochromic and Electroluminescence Materials. *Chem.—Eur. J.* **2022**, *28*, e202200826.
(31) dos Santos, P. L.; Stachelek, P.; Takeda, Y.; Pander, P. Recent Advances in Highly-Efficient Near Infrared OLED Emitters. *Mater. Chem. Front.* **2024**, *8*, 1731−1766.
(32) Pereira, D. de S.; Dos Santos, P. L.; Ward, J. S.; Data, P.; Okazaki, M.; Takeda, Y.; Minakata, S.; Bryce, M. R.; Monkman, A. P. An Optical and Electrical Study of Full Thermally Activated Delayed Fluorescent White Organic Light-Emitting Diodes. *Sci. Rep.* **2017**, *7*, 6234.
(33) Slater, J. C. Atomic Radii in Crystals. *J. Chem. Phys.* **1964**, *41*, 3199−3204.
(34) Data, P.; Okazaki, M.; Minakata, S.; Takeda, Y. Thermally Activated Delayed Fluorescence *vs.* Room Temperature Phosphorescence by Conformation Control of Organic Single Molecules. *J. Mater. Chem. C* **2019**, *7*, 6616−6621.
(35) Takeda, Y.; Mizuno, H.; Okada, Y.; Okazaki, M.; Minakata, S.; Penfold, T.; Fukuhara, G. Hydrostatic Pressure controlled Ratiometric Luminescence Responses of a Dibenzo[*a,j*]phenazine-Cored Mechanoluminophore. *ChemPhotoChem.* **2019**, *3*, 1203−1211.
(36) Enjou, T.; Goto, S.; Liu, Q.; Ishiwari, F.; Saeki, A.; Uematsu, T.; Ikemoto, Y.; Watanabe, S.; Matsuba, G.; Ishibashi, K.; Watanabe, G.; Minakata, S.; Sagara, Y.; Takeda, Y. Water-Dispersible Donor-Acceptor-Donor π-Conjugated Bolaamphiphiles Enabling a Humidity-Responsive Luminescence Color Change. *Chem. Commun.* **2024**, *60*, 3653−3656.
(37) Maillard, J.; Klehs, K.; Rumble, C.; Vauthey, E.; Heilemann, M.; Fürstenberg, A. Universal Quenching of Common Fluorescent Probes by Water and Alcohols. *Chem. Sci.* **2021**, *12*, 1352−1362.
(38) Yamagishi, H.; Nakajima, S.; Yoo, J.; Okazaki, M.; Takeda, Y.; Minakata, S.; Albrecht, K.; Yamamoto, K.; Badía-Domínguez, I.; Oliva, M. M.; Delgado, M. C. R.; Ikemoto, Y.; Sato, H.; Imoto, K.; Nakagawa, K.; Tokoro, H.; Ohkoshi, S.-I.; Yamamoto, Y. Sigmoidally Hydrochromic Molecular Porous Crystal with Rotatable Dendrons. *Commun. Chem.* **2020**, *3*, 118.
(39) Chen, Z.; Ho, C.-L.; Wang, L.; Wong, W. Y. Single-Molecular White-Light Emitters and Their Potential WOLED Applications. *Adv. Mater.* **2020**, *32*, 1903269.
(40) Sun, Y.; Giebink, N. C.; Kanno, H.; Ma, B.; Thompson, M. E.; Forrest, S. R. Management of Singlet and Triplet Excitons for Efficient White Organic Light-Emitting Devices. *Nature* **2006**, *440*, 908−912.
(41) Sasabe, H.; Kido, J. Recent Progress in Phosphorescent Organic Light-Emitting Devices. *Eur. J. Org. Chem.* **2013**, *2013*, 7653−7663.
(42) Bergamini, G.; Fermi, A.; Botta, C.; Giovanella, U.; Di Motta, S.; Negri, F.; Peresutti, R.; Gingras, M.; Ceroni, P. A Persulfurated Benzene Molecule Exhibits Outstanding Phosphorescence in Rigid Environments: From Computational Study to Organic Nanocrystals and OLED Applications. *J. Mater. Chem. C* **2013**, *1*, 2717−2724.
(43) Chaudhuri, D.; Sigmund, E.; Meyer, A.; Röck, L.; Klemm, P.; Lautenschlager, S.; Schmid, A.; Yost, S. R.; Van Voorhis, T.; Bange, S.; Höger, S.; Lupton, J. M. Metal-Free OLED Triplet Emitters by Side-Stepping Kasha's Rule. *Angew. Chem. Int. Ed.* **2013**, *52*, 13449−13452.
(44) Kabe, R.; Notsuka, N.; Yoshida, K.; Adachi, C. Afterglow Organic Light-Emitting Diode. *Adv. Mater.* **2016**, *28*, 655−660.
(45) Zhan, G.; Liu, Z.; Bian, Z.; Huang, C. Recent Advances in Organic Light-Emitting Diodes Based on Pure Organic Room Temperature Phosphorescence Materials. *Front Chem.* **2019**, *7*, 305.
(46) Hosono, T.; Decarli, N. O.; Crocomo, P. Z.; Goya, T.; de Sousa, L. E.; Tohnai, N.; Minakata, S.; de Silva, P.; Data, P.; Takeda, Y. The Regioisomeric Effect on the Excited-State Fate Leading to Room-Temperature Phosphorescence or Thermally Activated Delayed Fluorescence in a Dibenzophenazine-Cored Donor-acceptor-donor System. *J. Mater. Chem. C* **2022**, *10*, 4905−4913.
(47) Yamaguchi, S.; Akiyama, S.; Tamao, K. Colorimetric Fluoride Ion Sensing by Boron-Containing π-Electron Systems. *J. Am. Chem. Soc.* **2001**, *123*, 11372−11375.
(48) Yamaguchi, S.; Shirasaka, T.; Akiyama, S.; Tamao, K. Dibenzoborole-Containing π-Electron Systems: Remarkable Fluorescence Change Based on the "On/off" Control of the p_π-π^* Conjugation. *J. Am. Chem. Soc.* **2002**, *124*, 8816−8817.
(49) Liu, X. Y.; Bai, D. R.; Wang, S. Charge-Transfer Emission in Nonplanar Three-Coordinate Organoboron Compounds for Fluorescent Sensing of Fluoride. *Angew. Chem. Int. Ed.* **2006**, *45*, 5475−5478.
(50) Hudson, Z. M.; Wang, S. Impact of Donor-Acceptor Geometry and Metal Chelation on Photophysical Properties and Applications of Triarylboranes. *Acc. Chem. Res.* **2009**, *42*, 1584−1596.
(51) Wade, C. R.; Broomsgrove, A. E. J.; Aldridge, S.; Gabbaï, F. P. Fluoride Ion Complexation and Sensing Using Organoboron Compounds. *Chem. Rev.* **2010**, *110*, 3958−3984.
(52) Li, S.-Y.; Sun, Z.-B.; Zhao, C.-H. Charge-Transfer Emitting Triarylborane π-Electron Systems. *Inorg. Chem.* **2017**, *56*, 8705−8717.
(53) Nyga, A.; Izumi, S.; Higginbotham, H. F.; Stachelek, P.; Pluczyk, S.; de Silva, P.; Minakata, S.; Takeda, Y.; Data, P. Electrochemical and Spectroelectrochemical Comparative Study of Macrocyclic Thermally Activated Delayed Fluorescent Compounds: Molecular Charge Stability vs OLED EQE Roll off. *Asian J. Org. Chem.* **2020**, *9*, 2153−2161.
(54) Thom, K. A.; Nolden, O.; Weingart, O.; Izumi, S.; Minakata, S.; Takeda, Y.; Gilch, P. Femtosecond Spectroscopy on a Dibenzophenazine-Cored Macrocycle Exhibiting Thermally Activated Delayed Fluorescence. *ChemistryOpen* **2023**, *12*, e202300026.
(55) Izumi, S.; Nyga, A.; de Silva, P.; Tohnai, N.; Minakata, S.; Data, P.; Takeda, Y. Revealing Topological Influence of Phenylenediamine Unit on Physicochemical Properties of Donor-Acceptor-Donor-

https://doi.org/10.1021/acs.accounts.4c00353
Acc. Chem. Res. 2024, 57, 2219−2232

Acceptor Thermally Activated Delayed Fluorescent Macrocycles. *Chem.—Asian J.* **2020**, *15*, 4098−4103.
(56) Forgan, R. S.; Sauvage, J.-P.; Stoddart, J. F. Chemical Topology: Complex Molecular Knots, Links, and Entanglements. *Chem. Rev.* **2011**, *111*, 5434−5464.

https://doi.org/10.1021/acs.accounts.4c00353
Acc. Chem. Res. 2024, 57, 2219−2232